



# Resonant Excitation of Terahertz Surface Plasmons by Optical Rectification Over a Rippled Graphene Surface

Rohit Kumar Srivastav<sup>1</sup>

Received: 22 May 2024 / Accepted: 16 July 2024

© The Author(s), under exclusive licence to Springer Science+Business Media, LLC, part of Springer Nature 2024

## Abstract

Resonant excitation of terahertz surface plasmons by optical rectification over rippled graphene surface, deposited on SiO<sub>2</sub> using a mode conversion of amplitude modulated p-polarized laser beam. A pump surface plasmons exert a ponderomotive force on the free electrons of the graphene surface and impart a linear oscillatory velocity at the modulation frequency. The current density develops by coupling the linear oscillatory velocity with modulated electron density and resonantly excites the terahertz surface plasmons at the modulation frequency. The amplitude of terahertz surface plasmons can be tunable by Fermi energy of graphene surface  $E_F$ . There is a possibility that the current study will be used to utilize THz detectors and sensors.

**Keywords** Graphene · Terahertz · Surface plasmon · Optical rectification · Fermi energy

## Introduction

Terahertz (THz) technology has garnered significant academic attention in recent years owing to its expanding range of applications in fields such as sensing [1–3], medical imaging [4, 5], and communications [6, 7]. THz radiation is generated by various processes, such as the nonlinear mixing of two lasers [8, 9], optical rectification (OR) [10, 11], laser (or electron beam)-plasma interaction [12, 13], and photoconductive antennas [14, 15].

There is presently a significant focus on the investigation of graphene's potential applications, driven by its remarkable electronic, mechanical, and optical characteristics [16]. In particular, the development of graphene-based devices in the terahertz (THz) regime has garnered attention due to recent discoveries regarding the tunability of surface plasmons (SPs) supported by graphene sheets. This tunability can be achieved by adjusting the external gate voltage or through chemical doping [17, 18]. THz SPs generation over a rippled graphene surface studied using linear mode conversion and second harmonic by Srivastav and Panwar [19, 20]. Li et al. [21] investigated harmonic THz SPs generation

by electron beam over a uniform graphene surface. Bhasin and Tripathi [22] reported excitation of THz SPs on metallic surfaces by OR. Bhasin and Tripathi [23] investigated THz radiation generation by OR in magnetized rippled density plasma using an x-mode laser. Also, Singh et al. [24] theoretically studied the excitation of THz radiation by OR in transversely magnetized rippled density plasma using a hyperbolic-secant laser pulse. Generation of THz radiation over carbon nanotubes can be achieved using various laser profiles, such as self-focusing lasers and cross-focused Gaussian lasers, both in the presence and absence of a magnetic field [25–30]. Unadkat and Kumar [31] reported the generation of sub-THz radiation by an electron beam within the drift space of a plasma-assisted slow wave structure using particle-in-cell simulation.

This paper presents an analytical and numerical study of the excitation of THz SPs over a rippled graphene surface using a modulated amplitude of a p-polarized laser beam by OR (see Fig. 1). The excitation of SPs may be accomplished by the utilization of an amplitude-modulated p-polarized laser, obliquely incident at an angle on the interface between graphene and free space. This objective may be accomplished through two methods: the attenuated total reflection configuration or by directly irradiating the laser onto a rippled graphene surface that possesses a certain wave number. SPs wave, which is modulated amplitude exerts a ponderomotive force on free electrons in graphene. This ponderomotive force imparts oscillatory velocity to free electrons at

✉ Rohit Kumar Srivastav  
physicsrohit93@gmail.com

<sup>1</sup> Department of Physics and Materials Science and Engineering, Jaypee Institute of Information Technology, A-10, Noida 201307, Uttar Pradesh, India

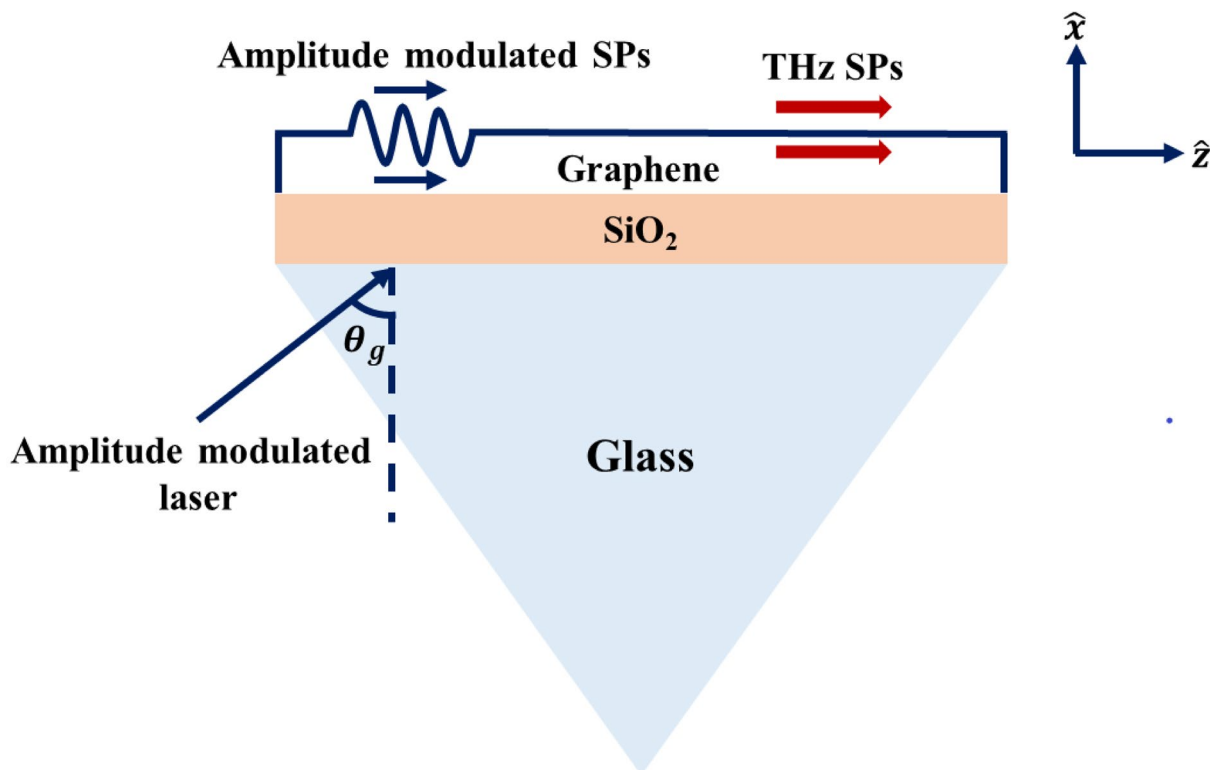


**Fig. 1** (Color Online) Schematic diagram of THz SPs generation by linear mode conversion of amplitude modulated laser (p-polarized)

the modulation frequency. The current density is produced by coupling oscillatory velocity with modulated electron density and resonant excitation of THz SPs at the modulation frequency. The linear current density is represented in “Linear Current Density” section. The expression of THz SPs is represented in “Terahertz Graphene Surface Plasmons Amplitude” section. Results and discussion in “Results and Discussion” section and conclusion in “Conclusion” section.

### Linear Current Density

The electric field of SPs wave is given as follows [22]:

$$\vec{E} = E e^{-i(\omega t - k_z z)} \begin{cases} (\hat{z} + \gamma_1 \hat{x}) e^{-\alpha_1 x}, & \text{for } x > 0 \\ (\hat{z} + \gamma_2 \hat{x}) e^{\alpha_2 x}, & \text{for } x \leq 0 \end{cases} \quad (1)$$

where  $E = E_0(1 + \mu \cos \Omega(t - z/v_g))$ ,  $\alpha_1^2 = (k_z^2 - (\omega^2/c^2))$ ,  $\alpha_2^2 = k_z^2 - (\omega^2/(c^2 \epsilon_{eff}))$ ,  $\gamma_1 = -(ik_z/\alpha_1)$ ,  $\gamma_2 = -(ik_z/\alpha_2)$ ,  $\epsilon_{eff}^\Omega = \epsilon_{SiO_2} + (i\sigma_g)/(\Omega \epsilon_0)$ ,  $\sigma_g = (ie^2 E_F)/(\pi \hbar^2 (\omega + i\nu))$  is conductivity of graphene,  $e$  is electron charge and  $\hbar$  is Plank constant,  $E_F$  is Fermi energy of graphene,  $\nu$  is collision frequency,  $k_z$  is propagation constant of SPs wave in direction of  $\hat{z}$ ,  $\mu$  is modulation index,  $\Omega$  is modulation frequency and  $v_g$  is group velocity of SPs wave.

The SPs electric field imparts oscillatory velocity  $\vec{v}_\omega$  to the electrons of the graphene surface, may be written as follows:

$$v_\omega^x = \frac{-i\gamma_2 e}{m_e^*(\omega + i\nu)} E e^{\alpha x} e^{-i(\omega t - k_z z)} \quad (2)$$

$$v_\omega^z = \frac{-ie}{m_e^*(\omega + i\nu)} E e^{\alpha x} e^{-i(\omega t - k_z z)} \quad (3)$$

where  $m_e^*$  is the effective mass,  $m_e^* = E_F/v_F^2$  [32] and  $v_F$  is Fermi velocity.

The SPs wave exerts ponderomotive force  $\vec{F}_p = -(m_e^*/4)(\vec{v}_s \cdot \nabla \vec{v}_s^* + \vec{v}_s^* \cdot \nabla \vec{v}_s) - (e/4)(\vec{v}_s \times \vec{B}_s^* + \vec{v}_s^* \times \vec{B}_s)$  on free electrons and it represented as follows:

$$\vec{F}_p = \frac{1}{4} \frac{e^2}{m_e^*} E^2 e^{(\alpha_2 + \alpha_1^*)x} (-F_{Px} \hat{x} + F_{Pz} \hat{z}) \quad (4)$$

where  $F_{Px} = (\tilde{v}_\omega^x \alpha_2^* \tilde{v}_\omega^{*x} - \tilde{v}_\omega^z ik_z \tilde{v}_\omega^{*z}) + (v_\omega^{*x} \alpha_2 \tilde{v}_\omega^x + v_\omega^{*z} ik_z \tilde{v}_\omega^z) + (1/i\omega)(\tilde{v}_\omega^{*z}(\alpha_2 - ik_z \beta_2) + \tilde{v}_\omega^z(\alpha_2^* + ik_z \beta_2^*))$  and  $F_{Pz} = (1/i\omega)(\tilde{v}_\omega^{*x}(\alpha_2 - ik_z \beta_2) + \tilde{v}_\omega^x(\alpha_2^* + ik_z \beta_2^*)) - ((\tilde{v}_\omega^x \alpha_2^* \tilde{v}_\omega^{*z} - \tilde{v}_\omega^z ik_z \tilde{v}_\omega^{*z}) + (v_\omega^{*x} \alpha_2 \tilde{v}_\omega^z + v_\omega^{*z} ik_z \tilde{v}_\omega^z))$

Considering the ponderomotive force at modulation frequency  $\Omega$  can be written as follows:

$$F_{p\Omega}^x = -\frac{e^2}{m_e^*} E_0^2 \mu F_{Px} e^{(\alpha_2 + \alpha_2^*)x} e^{-i\Omega \left( t - \frac{z}{v_g} \right)} \quad (5)$$

Now, the oscillatory velocity components of free electrons at modulation frequency  $\Omega$  is given as follows:

$$v_{\Omega}^x = \tilde{v}_{\Omega}^x \frac{e^2}{(m_e^*)^2} E_0^2 \mu e^{(\alpha_2 + \alpha_2^*)x} e^{-i\Omega \left( t - \frac{z}{v_g} \right)} \quad (6)$$

and

$$v_{\Omega}^z = 0 \quad (7)$$

where  $\tilde{v}_{\Omega}^x = iF_{Px}/(\Omega + iv)$ .

The oscillatory velocity couples with modulated electron density to produce current density  $\vec{J}_{\Omega}$  at modulation frequency  $\Omega$  and it is given as follows:

$$\vec{J}_{\Omega} = \frac{1}{2} n_0 \tilde{v}_{\Omega}^x \frac{e^3}{(m_e^*)^2} E_0^2 e^{(\alpha_2 + \alpha_2^*)x} e^{-i\Omega t} e^{i \left( \frac{\Omega}{v_g} + q \right) z} \mu h \delta(x) \hat{x} \quad (8)$$

### Terahertz Graphene Surface Plasmons Amplitude

By using Maxwell's equation,  $\Omega$  modulation frequency SPs wave field can be expressed as follows:

$$\vec{\nabla} \times \vec{E}_s = i\Omega \vec{B}_s \quad (9)$$

and

$$\vec{\nabla} \times \vec{B}_s = \vec{J}_{\Omega} - i\Omega \epsilon_0 \epsilon_{eff}^{\Omega} \vec{E}_s \quad (10)$$

where  $\epsilon_{eff}^{\Omega} = \epsilon_{SiO_2} + (i\sigma_g)/(\Omega \epsilon_0)$  for  $x \leq 0$  and  $\epsilon_{eff}^{\Omega} = 1$  for  $x > 0$ , and  $s$  represents the SPs.

The wave equation may be written as follows:

$$\vec{\nabla}^2 \vec{E}_s - \vec{\nabla}(\vec{\nabla} \cdot \vec{E}_s) - \frac{\Omega^2}{c^2} \left( \epsilon_{eff}^{\Omega} \vec{E}_s \right) = -\mu_0 i\Omega \vec{J}_{\Omega} \quad (11)$$

Here,  $\epsilon_{eff}^{\Omega}$  is graphene effective permittivity at frequency  $\Omega$ . When r.h.s term of Eq. (11) is zero that is  $\vec{J}_{\Omega}$  is absence then SPs eigen mode structure with

$$\vec{E}_s = \vec{E}_{s,0}, \vec{B}_s = \vec{B}_{s,0} \quad (12)$$

where  $\vec{E}_{s,0}$  and  $\vec{B}_{s,0}$  is given as follows:

$$\vec{\nabla} \times \vec{E}_{s,0} = i\Omega \vec{B}_{s,0} \quad (13)$$

and

$$\vec{\nabla} \times \vec{B}_{s,0} = -i\Omega \epsilon_0 \epsilon_{eff}^{\Omega} \vec{E}_{s,0} \quad (14)$$

The SPs electric field can be represented as follows:

$$\vec{E}_{s,0} = e^{-i(\Omega t - k_z^{\Omega} z)} \begin{cases} (\hat{z} + \gamma_1^{\Omega} \hat{x}) e^{-\alpha_1^{\Omega} x}, & \text{for } x > 0 \\ (\hat{z} + \gamma_2^{\Omega} \hat{x}) e^{\alpha_2^{\Omega} x}, & \text{for } x \leq 0 \end{cases} \quad (15)$$

where  $\gamma_1^{\Omega} = -(ik_z^{\Omega}/\alpha_1^{\Omega})$ ,  $\gamma_2^{\Omega} = -ik_z^{\Omega}/\alpha_2^{\Omega}$ ,  $(\alpha_2 k_z^{\Omega})^2 = (k_z^{\Omega})^2 - (\Omega^2/c^2)\epsilon_{eff}^{\Omega}$ ,  $(\alpha_1^{\Omega})^2 = (k_z^{\Omega})^2 - (\Omega^2/c^2)$ ,  $k_z^{\Omega} = q + \Omega/v_g$  and  $q$  provides the extra wave number for phase matching condition.

Figure 2 represents the variation of  $q$  with THz frequency  $\omega$  for different values of graphene Fermi energy  $E_F = 0.35\text{eV}$  (green line),  $E_F = 0.40\text{eV}$  (blue dashed line) and  $E_F = 0.45\text{eV}$  (red dotted line) at  $\Omega = 1\text{ THz}$ .

If the current density  $\vec{J}_{\Omega}$  is present, then the electric and magnetic fields of the THz SPs wave can be expressed as follows:

$$\vec{E}_s = a(t)\vec{E}_{s,0}, \vec{B}_s = b(t)\vec{B}_{s,0} \quad (16)$$

Solving Eqs. (10) and (11) with Eq. (16), and using Eq. (13), we get

$$(a - b)i\Omega \epsilon_0 \epsilon_{eff}^{\Omega} \vec{E}_{s,0} = \vec{J}_{\Omega} + \vec{E}_{s,0} \frac{\partial a}{\partial t} \epsilon_0 \epsilon_{eff} \quad (17)$$

and

$$b - a = \frac{1}{i\Omega} \frac{\partial b(t)}{\partial t} \quad (18)$$

Using Eq. (17) in Eq. (18) and taking  $\partial a/\partial t \approx \partial b/\partial t$ , we get

$$\frac{\partial a}{\partial t} \vec{E}_{s,0} = -\frac{1}{2\epsilon_0 \epsilon_{eff}^{\Omega}} \vec{J}_{\Omega} \quad (19)$$

Multiplying Eq. (19) by  $\vec{E}_{s,0}^* dx$  and integrate  $-\infty$  to  $\infty$ , we obtained

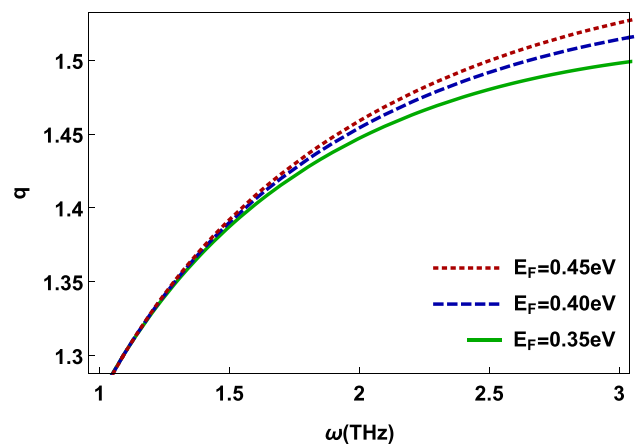


**Fig. 2** (Color Online) Variation of ripple wave number of  $q$  with THz frequency  $\omega$  for three values of graphene Fermi energy  $E_F = 0.35\text{eV}$  (green line),  $E_F = 0.40\text{eV}$  (blue dashed line) and  $E_F = 0.45\text{eV}$  (red dotted line)

$$\frac{\partial a}{\partial t} = -\frac{1}{2\epsilon_0\epsilon_{eff}^\Omega} \frac{I_2}{I_1} \quad (20)$$

where  $I_1 = \int_{-\infty}^{\infty} \vec{E}_{s,0} \cdot \vec{E}_{s,0}^* dx$  and  $I_2 = \int_{-\infty}^{\infty} \vec{J}_\Omega \cdot \vec{E}_{s,0}^* dx$ .

Solving Eq. (20), one may obtained

$$\frac{\partial a}{\partial t} = \frac{E_0^2 \mu h}{2\epsilon_{eff}^\Omega} \frac{n_0 e^3}{\epsilon_0 (m_e^*)^2} \frac{\tilde{\nu}_\Omega^x (\gamma_2^\Omega)^*}{\left(\frac{1+\gamma_2^2}{\alpha_2^\Omega} + \frac{1+\gamma_1^2}{\alpha_1^\Omega}\right)} \quad (21)$$

Let  $\partial/\partial t = -i\Omega$ , we obtain

$$\left| \frac{a}{E_0} \right| = \left| \frac{E_0 e h \mu \omega_p^2}{2i\Omega \epsilon_{eff}^\Omega m_e^*} \frac{\tilde{\nu}_\Omega^x (\gamma_2^\Omega)^*}{\left(\frac{1+\gamma_2^2}{\alpha_2^\Omega} + \frac{1+\gamma_1^2}{\alpha_1^\Omega}\right)} \right| \quad (22)$$

Equation (22) represents the THz SPs amplitude ratio  $|a/A_0|$ . It depends upon the ripple height  $h$ , modulation index  $\mu$ , and Fermi energy of graphene surface  $E_F$ .

## Results and Discussion

The ripple wave number  $q$  increases with an increase in Fermi energy of graphene surface  $E_F$  at particular values of THz frequency  $\omega$ . Also, the Ripple wave number  $q$  increases with an increase in THz frequency  $\omega$  at particular values of Fermi energy of graphene surface  $E_F$ . Ripple wave number  $q$  gives the extra wave number to resonantly excite the THz SPs wave. THz SPs amplitude ratio  $|a/A_0|$  verses THz frequency  $\omega$  is plotted in Fig. 3 for three values of graphene Fermi energy  $E_F = 0.35\text{eV}$  (green line),  $E_F = 0.40\text{eV}$  (red dashed line) and  $E_F = 0.45\text{eV}$  (blue dotted line) at  $\mu = 0.3$ ,  $h = 50\mu\text{m}$ ,  $\Omega = 2$  THz and  $\epsilon_{\text{SiO}_2} = 3.9$ . THz SPs amplitude increases with a decrease in THz frequency  $\omega$ . Also, it increases with a decrease in Fermi energy of graphene surface  $E_F$ .

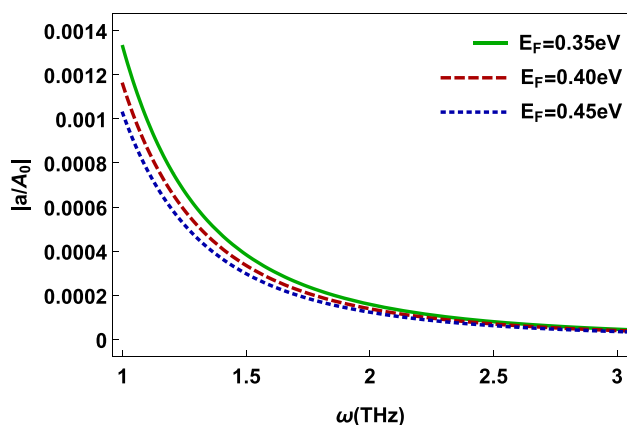


**Fig. 3** (Color Online) THz SPs amplitude ratio  $|a/A_0|$  verses THz frequency  $\omega$  for three values of graphene Fermi energy  $E_F = 0.35\text{eV}$  (green line),  $E_F = 0.40\text{eV}$  (red dashed line) and  $E_F = 0.45\text{eV}$  (blue dotted line). Other parameters are  $\mu = 0.3$ ,  $h = 50\mu\text{m}$  and  $\epsilon_{\text{SiO}_2} = 3.9$

## Conclusion

In the present paper, theoretically and numerically examined the generation of THz SPs over a rippled graphene surface through OR of an amplitude-modulated p-polarized laser. The generation of THz SPs was examined within the frequency range of 1 to 3 THz, with the Fermi energy of graphene  $E_F$  vary from 0.35 to 0.45 eV. The amplitude of THz SPs was found to increase as the THz frequency and Fermi energy of graphene decreased. Additionally, the amplitude of THz SPs increased with an increase in the modulation index, ripple height, and laser amplitude. This work explores the potential use of the Fermi energy of graphene to control the excitation of THz waves at specific frequencies, thereby enabling the development of THz devices [33–35].

**Author Contributions** Rohit Kumar Srivastav developed the formulation of the manuscript. Rohit Kumar Srivastav prepared Figs. 1–3.

**Funding** The authors have not disclosed any funding.

**Data Availability** No datasets were generated or analyzed during the current study.

## Declarations

**Ethical Approval** This declarations is “not applicable.”

**Competing Interests** The authors declare no competing interests.

## References

1. Gezimati M, Singh G (2023) Terahertz imaging and sensing for healthcare: current status and future perspectives. *IEEE Access* 11:18590–18619
2. Hillger P, Grzyb J, Jain R, Pfeiffer UR (2019) Terahertz imaging and sensing applications with silicon-based technologies. *IEEE Trans Terahertz Sci Technol* 9(1):1–19
3. Bogue R (2018) Sensing with terahertz radiation: a review of recent progress. *Sens Rev* 38(2):216–222
4. Castro-Camus E, Koch M, Mittleman DM (2022) Recent advances in terahertz imaging: 1999 to 2021. *Appl Phys B* 128(1):12
5. Yang X, Zhao X, Yang K, Liu Y, Liu Y, Fu W, Luo Y (2016) Biomedical applications of terahertz spectroscopy and imaging. *Trends Biotechnol* 34(10):810–824
6. Huang Y, Shen Y, Wang J (2023) From terahertz imaging to terahertz wireless communications. *Engineering* 22:106–124
7. Banafaa M, Shayea I, Din J, Azmi MH, Alashbi A, Daradkeh YI, Alhammadi A (2023) 6g mobile communication technology: requirements, targets, applications, challenges, advantages, and opportunities. *Alex Eng J* 64:245–274
8. Kumar M, Lee K, Hee Park S, Uk Jeong Y, Vinokurov N (2017) Terahertz radiation generation by nonlinear mixing of two lasers in a plasma with density hill. *Phys Plasmas* 24(3):033104
9. Chauhan S, Parashar J (2014) Laser beat wave excitation of terahertz radiation in a plasma slab. *Phys Plasmas* 21(10):103113

10. Singh RK, Singh M, Rajouria SK, Sharma R (2017) High power terahertz radiation generation by optical rectification of a shaped pulse laser in axially magnetized plasma. *Phys Plasmas* 24(10):103103
11. Kumar S, Singh RK, Sharma R (2016) Strong terahertz generation by optical rectification of a super-gaussian laser beam. *Europhys Phys Rev Lett* 114(5):55003
12. Gupta D, Jain A, Kulagin V, Hur MS, Suk H (2022) Coherent terahertz radiation generation by a flattened gaussian laser beam at a plasma-vacuum interface. *Appl Phys B* 128(3):50
13. Yang S, Wang S, Wang Z, Zhang P, Xia Y, Tang C, Gong Y (2022) Terahertz radiation generated by electron-beam-driven plasma waves in a transverse external magnetic field. *Phys Plasmas* 29(5):053106
14. Shalini M, Madhan MG (2022) Photoconductive bowtie dipole antenna incorporating photonic crystal substrate for terahertz radiation. *Opt Commun* 517:128327
15. Bobby ENF, Prajapati J, Rathinasamy V, Rao TR, Mondal S (2022) 6g and beyond: investigation of broadband terahertz interdigitated photoconductive antenna by exploiting laser parameters. *Microw Opt Technol Phys Rev Lett* 64(12):2197–2206
16. Novoselov KS, Geim AK, Morozov SV, Jiang DE, Zhang Y, Dubonos SV, Grigorieva IV, Firsov AA (2004) Electric field effect in atomically thin carbon films. *Science* 306(5696):666–669
17. Yarahmadi M, Moravvej-Farshi MK, Yousefi L (2015) Subwavelength graphene-based plasmonic thz switches and logic gates. *IEEE Trans Terahertz Sci Technol* 5(5):725–731
18. Liu M, Yin X, Ulin-Avila E, Geng B, Zentgraf T, Ju L, Wang F, Zhang X (2011) A graphene-based broadband optical modulator. *Nature* 474(7349):64–67
19. Srivastav RK, Panwar A (2023) Linear mode conversion of terahertz radiation into terahertz surface plasmon wave over a graphene-free space interface. *Int J Mater Res* 114(7–8):572–578
20. Srivastav RK, Panwar A (2023) Generation of second harmonic terahertz surface plasmon wave over a rippled graphene surface. *Int J Mater Res* 114(7–8):579–585
21. Li D, Wang Y, Nakajima M, Hashida M, Wei Y, Miyamoto S (2016) Harmonics radiation of graphene surface plasmon polaritons in terahertz regime. *Phys Phys Rev Lett A* 380(25–26):2181–2184
22. Bhasin L, Tripathi VK (2010) Resonant terahertz generation by optical rectification of an amplitude modulated surface plasma wave. *IEEE J Quantum Electron* 46(6):965–969
23. Bhasin L, Tripathi VK (2009) Terahertz generation via optical rectification of x-mode laser in a rippled density magnetized plasma. *Phys Plasmas* 16(10):103105
24. Singh RK, Singh M, Rajouria SK, Sharma R (2017) Strong terahertz emission by optical rectification of shaped laser pulse in transversely magnetized plasma. *Phys Plasmas* 24(7):073114
25. Kumar S, Vij S, Kant N (2022) Combined effect of transverse electric and magnetic fields on THz generation by beating of two amplitude-modulated laser beams in the collisional plasma. *J Astrophys Astron* 43:30
26. Kumar S, Vij S, Kant N (2022) Interaction of obliquely incident lasers with anharmonic CNTs acting as dipole antenna to generate resonant THz radiation. *Waves in Random and Complex Media* 1-13
27. Kumar S, Vij S, Kant N (2022) Resonant terahertz generation by the interaction of laser beams with magnetized anharmonic carbon nanotube array. *Plasmonics* 17:381–388
28. Kumar S, Vij S, Kant N, Thakur V (2022) Resonant terahertz generation by cross-focusing of Gaussian laser beams in the array of vertically aligned anharmonic and magnetized CNTs. *Opt Commun* 513:128112
29. Thakur V, Kant N, Kumar S (2023) THz field enhancement under the influence of cross-focused laser beams in the m-CNTs. *Trends Sci* 20(6):5284
30. Kumar S, Kant N, Thakur V (2023) THz generation by self-focused Gaussian laser beam in the array of anharmonic VA-CNTs. *Opt Quant Electron* 55:281
31. Unadkat P, Kumar N (2024) Study of space charge potential for propagation of plasma-assisted electron beam. In: *IEEE Transactions on Plasma Science* 1-7
32. Verma N, Govindan A, Kumar P (2021) Terahertz plasmon excitation by nonlinear mixing of two laser beams in graphene sheet. *Plasmonics* 16(3):711–716
33. Sandeep HK (2023) Malik, enhancement of terahertz radiation due to excitation of spw on graphene strip coated on GaAs structure. *Results Opt* 13:100538
34. Shur M (2024) Sensing using terahertz radiation. *Int J High Speed Electron Syst* 2440022
35. Islam M, Bhardwaj A, Kumar G (2024) Planar terahertz multi-resonator meta-waveguide based upon strongly coupled nested split-ring resonator. *Optik* 302:171712

**Publisher's Note** Springer Nature remains neutral with regard to jurisdictional claims in published maps and institutional affiliations.

Springer Nature or its licensor (e.g. a society or other partner) holds exclusive rights to this article under a publishing agreement with the author(s) or other rightsholder(s); author self-archiving of the accepted manuscript version of this article is solely governed by the terms of such publishing agreement and applicable law.